

# Absorption of Thermal Radiation by Burning Polymers

Gregory Linteris<sup>1</sup>, Mauro Zammarano<sup>1</sup>, Boris Wilthan<sup>2</sup>, Leonard Hanssen<sup>2</sup>

<sup>1</sup>Fire Science Division    <sup>2</sup>Optical Technology Division  
National Institute of Standards and Technology, USA

## ABSTRACT

In large-scale fires, the input of energy to burning materials occurs predominantly by radiative transfer. The in-depth absorption of radiant energy by a polymer influences its ignition time and burning rate. The present investigation examines two methods for obtaining the absorption coefficient of polymers for infrared radiation from high-temperature sources: a broadband method and a spectral method. Data on the broadband absorption coefficient for two thermoplastics, poly(methyl methacrylate) and polyoxymethylene are presented, and they are found to vary with thickness. Implications for modeling of mass loss experiments are discussed.

**KEYWORDS:** pyrolysis modeling, material flammability, IR absorption

## INTRODUCTION

The absorption of radiation in semi-transparent media is a complex but well-studied phenomena<sup>1</sup>. In-depth absorption of radiation has application to ablative materials for reentry bodies and hypersonic vehicles<sup>2</sup>, thermoforming and processing of polymers<sup>3,6</sup>, thin-film glazing for solar thermal systems<sup>7</sup>, and the prediction of polymer burning rates in fires<sup>8,10</sup>.

In fire research, the in-depth absorption of radiation is important for material ignition as well as for fire growth and spread<sup>11</sup>. When subjected to a known radiant flux, the polymer's time to ignition and subsequent mass loss rate are controlled primarily by the material's thermodynamic and chemical kinetic properties related to decomposition, as well as by those related to the transfer of heat into the material (such as the density, thermal conductivity and specific heat)<sup>12</sup>. For semi-transparent materials, in-depth absorption of radiation, diathermicity, is also important<sup>13</sup>. Moreover, accurate knowledge of the absorption of the radiation is required for validation of models of material decomposition<sup>14,15</sup>.

Recently, the in-depth absorption of radiation has been shown to have a large effect on the time to ignition for poly(methyl methacrylate) (PMMA) subjected to a high ( $> 100 \text{ kW/m}^2$ ) radiant flux<sup>16</sup>. In that reference, Jiang et al. measured the absorption coefficient of black PMMA with a broadband source and detector, and developed an analytical model for predicting the ignition time. The model was able to predict well the ignition time measured in earlier experiments<sup>17</sup>. In other work, the effect of IR transmission in the polymer on the time to ignition has been calculated for a polymer slab, of varying decomposition rates and absorption coefficients, subjected to varying radiant fluxes<sup>18</sup>. For example, Figure 1 shows the ignition time for a 25.4 mm thick slab of PMMA as a function of the imposed radiant flux, with total average (integrated over all wavelengths) absorption coefficient varied from  $200 \text{ m}^{-1}$  to  $50000 \text{ m}^{-1}$ <sup>18</sup>. As indicated, this variation in the absorption coefficient gives a factor of two difference in the ignition time at low flux, and a eleven at high flux. In addition to the ignition time, the burning characteristics of the PMMA are changed as well, so that for model validation, the value of the absorption coefficient can be important<sup>18</sup>.

The goal of the present work is to examine several methods of obtaining the required average absorption coefficient for polymers exposed to the radiant flux typical of fires, so that the value of that parameter can be input into numerical models of fire growth, such as the Fire Dynamics Simulator (FDS)<sup>19</sup> GPyro<sup>12</sup> or ThermaKin<sup>20</sup>. As described below, two methods are used to study the absorption of IR by thermoplastic polymers. The first is based on the NIST Gasification Device (GD)<sup>21</sup>, and the second, on the NIST integrating-sphere (IS) system with a Fourier transform (FT) spectrophotometer<sup>22</sup>.

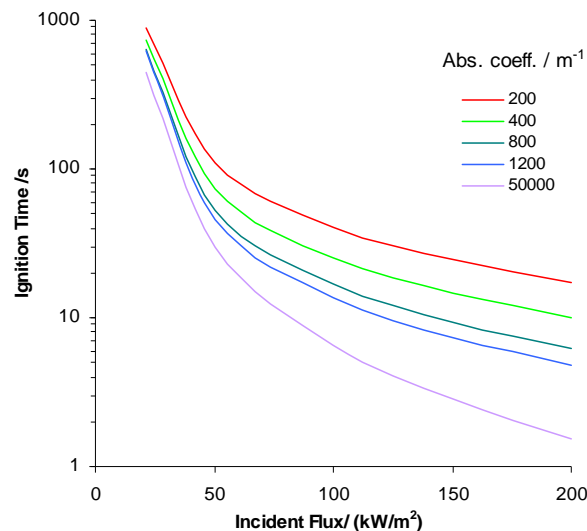


Figure 1– Ignition time as a function of the radiant flux, for a 25.4 mm thick sample of PMMA with varying values of the absorption coefficient (from<sup>18</sup>).

## EXPERIMENT

### NIST Gasification Device

The NIST gasification device has been described previously<sup>21</sup>. In the present work, a cone-shaped resistive heater at  $(1081 \pm 1)$  K and located in a water-cooled, nitrogen-purged chamber, irradiates the horizontal polymer specimen located 14 cm from the heater bottom. The 50 mm x 50 mm square polymer sheets are placed horizontally and centered on top of a vertical stainless steel tube (2.54 cm diameter). Concentric in the tube, and located 1 cm below the polymer sample is a calibrated heat flux gage (Medterm model GTW-732-485A), which monitors the broad-band radiation transmitted through the sample. A water-cooled shutter, positioned between the cone heater and the sample, blocks radiation until a test is initiated, whereupon the shutter is removed, and the data are collected for about 5 s, and the shutter replaced. The measurements in the NIST gasification device are performed using an approach similar to that in ref. <sup>16</sup>; however, the NIST device does not attempt to conductively cool the sample.

### Integrating-Sphere Device

The NIST integrating-sphere device has been described previously<sup>22</sup>. A modulated beam from an FT infrared interferometer passes through the material, which is mounted on the sample port of an integrating sphere. An InSb detector with a non imaging concentrator, also mounted on the integrating sphere, monitors either the reflected or transmitted energy through the sample and a ratio to the reference beam through the empty reference port of the sphere is computed. The value of the spectral transmittance  $\tau_{\lambda}$ , or spectral reflectance  $\rho_{\lambda}$ , for the sample of thickness  $S$ , is measured directly for the sensitive wavelength range of the detector (1.5  $\mu\text{m}$  to 15.1  $\mu\text{m}$ ). While both, the total and diffuse components of the transmitted and reflected light are obtained (the specular component can be computed from measured data), only the total of the near normal ( $8^\circ$ ) directional hemispherical reflectance/transmittance values are reported in the present work for comparison with the results obtained using the NIST gasification device.

## Materials

Two typical commodity polymers were used: black poly(methyl methacrylate), PMMA (Polycast<sup>1</sup>), as in ref. <sup>16</sup> and polyoxymethylene, POM, as in ref. <sup>23</sup> (both from the same sample batch, and provided by the authors of those references). The samples were prepared by hot pressing to the desired thickness. The actual thickness of all the samples was subsequently determined as the average of five measurements with a micrometer in the central region, corresponding to the optical path.

## Uncertainties

All uncertainties are reported as *expanded uncertainties*:  $X \pm ku_c$ , from a combined standard uncertainty (estimated standard deviation)  $u_c$ , and a coverage factor  $k$  as described. Likewise, when reported, the relative uncertainty is  $ku_c/X$ . The only measured parameters are the material thickness and the transmitted and reflected (in the case of the IS) intensity. The uncertainty (type B) in the thickness arises primarily from variation in the material thickness in the region of the measurement. In the central (6 mm diameter) portion of the samples where the transmission measurements were taken, the relative uncertainty (66 % confidence level,  $k=1$ ) is 3 % for the POM and PMMA samples (except the 0.47 mm POM, and 0.093, 0.109, and 0.178) mm PMMA samples, for which the relative uncertainty was (11, 8, 6, 10) %. In the NIST gasification device, the combined relative uncertainty (type B) on the transmittance is estimated to be 5 % ( $k=1$ ), mostly from correction from the polymer re-radiation, as described in the results section below. In the NIST Integrating Sphere Device, the combined relative uncertainty for the spectral transmittance or reflectance for PMMA, which is specular, is 0.3 % ( $k=2$ ); while for POM, which is diffuse, it is 3 %.

## DATA ANALYSIS

The attenuation of radiation in a medium is described by Bouguer's law:

$$\frac{i_{\lambda}'(S)}{i_{\lambda}'(0)} = \exp\left[-\int_0^S K_{\lambda}(S^*)dS^*\right] \quad [1]$$

in which  $i$  is the radiation intensity,  $K$  is the extinction coefficient,  $S$  is the path length through the medium, and the subscripts  $\lambda$  and  $'$  denote spectral and directional <sup>1</sup>. The extinction coefficient is composed of two parts, an absorption coefficient  $a_{\lambda}(\lambda)$  and a scattering coefficient  $\sigma_{s\lambda}(\lambda)$ :

$$K_{\lambda} = a_{\lambda}(\lambda) + \sigma_{s\lambda}(\lambda) \quad [2]$$

The inverse of the extinction coefficient is the mean penetration depth of the radiation ( $l_m = 1/K_{\lambda}$ ). For the present conditions, the scattered light is assumed to be quickly absorbed, so that  $K_{\lambda} \approx a_{\lambda}$ , and assuming isotropic behavior,  $a_{\lambda}$  does not vary with  $S$ , so Bouguer's law becomes:

$$\tau_{\lambda}' = \frac{i_{\lambda}'(S)}{i_{\lambda}'(0)} = e^{-a_{\lambda}S} \quad [3]$$

in which  $\tau_{\lambda}'$  is the directional spectral transmittance for the path length  $S$ .

Ultimately, we seek to obtain an average value (over all wavelengths) and total values (sum of directional and diffuse) for the absorptance,  $a$ , which is what is used to describe radiation transport in the material by

---

<sup>1</sup> Certain commercial equipment, instruments, and materials are identified in this paper to adequately specify the procedure. Such identification does not imply recommendation or endorsement by the National Institute of Standards and Technology.

the three most common sub-grid models for material decomposition in fires<sup>12,19,20</sup>. In the transmission experiments using the cone heater in the NIST gasification device, the incident radiation is spectrally broad, and is assumed to follow a blackbody distribution at the heater temperature. Hence, the measurements represent the average (not spectral) transmittance. Also, the configuration does not distinguish between the diffuse and specular components of the transmitted radiation. As a result, the NIST gasification device measures the average total transmittance, from which average total absorptance  $a$  can be determined. For a thin sample, with the inclusion of the front and back reflective surfaces (and neglecting the effects of multiple reflections), the average total transmittance through a thin sheet of material becomes:

$$\tau(S) = (1 - \rho)^2 e^{-aS} \quad [4]$$

in which  $\rho$  is the average reflectance of each surface. This can be re-written as:

$$\ln[\tau(S)] = 2 \ln[1 - \rho] - aS \quad [5]$$

so that a plot of  $-\ln[\tau(S)]$  versus  $S$  has a slope of  $a$  and an intercept of  $-2 \ln[1 - \rho]$ .

In the case of the NIST IS, the directional (or total) spectral transmittance  $\tau'_\lambda(\lambda)$  is measured directly for a given thickness of material. To obtain the average total absorptance  $a$  from the measurements in the IS, we seek to average over the conditions of the measurements in the NIST gasification device (with which we will compare the IS measurements). Hence, we use the IS-measured total spectral transmittance  $\tau_\lambda(\lambda, S)$  and average this over the spectral distribution of the incident radiation from the NIST gasification device cone heater. The average total transmittance for a sample of thickness  $S$   $\tau(S)$  is then given by:

$$\tau(S) = \frac{\int_0^\infty \tau_\lambda(\lambda, S) i'_\lambda(0) d\lambda}{\int_0^\infty i'_\lambda(0) d\lambda} \quad [6]$$

in which the incident spectral radiation intensity  $i'_\lambda(0)$  is approximated as that of a black body in a vacuum at the measured heater temperature. Using Planck's spectral distribution

$$i'_\lambda(0) = i'_{\lambda b}(\lambda) = \frac{2C_1}{\lambda^5 (e^{C_2/\lambda T} - 1)} \quad [7]$$

(with  $C_1=0.59544 \times 10^{-16} \text{ W m}^2$  and  $C_2=14388 \text{ } \mu\text{m K}^{-1}$ ) provides  $\tau(S)$ , and the resulting data can be plotted as  $-\ln[\tau(S)]$  versus  $S$  to yield  $a$  as the slope.

The reflectance can also be illustrated via the plots of  $-\ln[\tau(S)]$  versus  $S$ . As indicated above, the intercept of the curve (i.e., zero thickness) is  $-2 \ln[1 - \rho]$ . In the IS measurements, the diffuse, directional, and total reflectance are obtained for each sample thickness of each of the two polymers. To calculate the average total reflectance  $\rho(S)$ , the total spectral reflectance  $\rho_\lambda(\lambda, S)$  is substituted for the total spectral transmittance  $\tau_\lambda(\lambda)$  in Eq. 6 above. For these polymer films, the normal incidence average

total reflectance  $\rho$  can also be estimated <sup>7</sup> based on the real part of the index of refraction in the visible ( $n_f$ ):

$$\rho = \left( \frac{n_f - 1}{n_f + 1} \right)^2 \quad [8]$$

## RESULTS

For the NIST gasification device, typical time-traces of the measured heat flux through four thicknesses of POM are shown in Figure 2. In that figure, the incident heat flux (in the absence of polymer sample) is 35.8 kW/m<sup>2</sup>. As indicated, after the shutter is removed and the flux-gage transient occurs (about 1 s), the flux increases with time (due to absorption of radiation, polymer heating, and subsequent re-radiation); the effect is larger for thinner samples (which heat faster). In the data analysis, the value of the transmitted flux in the absence of polymer heating is obtained by extrapolating the increasing flux back (three points) to the time where the shutter is removed (as indicated near the rising part of the curve for S=0.37 in Figure 2). The uncertainty in this value is estimated to be one half the correction due to the extrapolation.

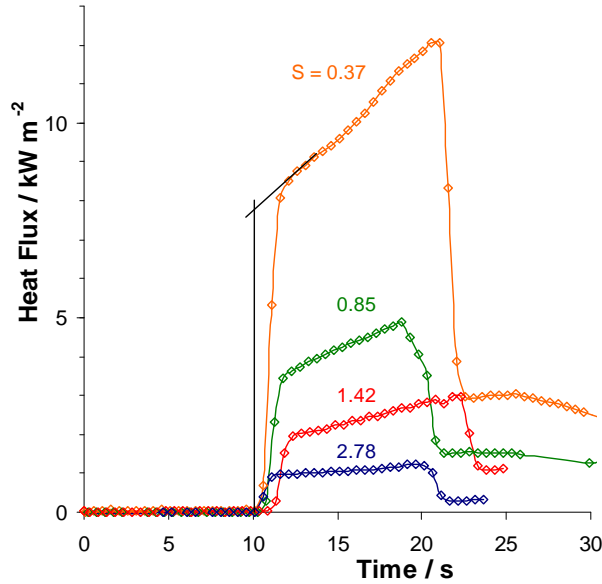


Figure 2 - Time history of heat flux through the back face of a clear sheet of POM (for four sample thicknesses), with the front face exposed to an incident flux is 35.8 kW/m<sup>2</sup>.

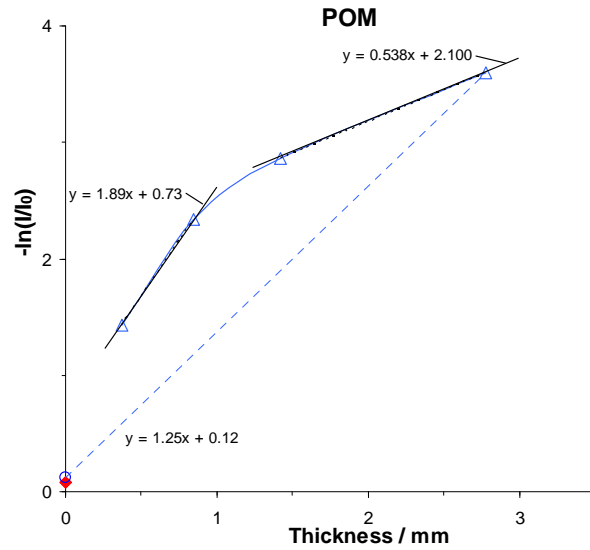


Figure 3 -  $-\ln(I/I_0)$  vs thickness for POM (GD).

From the gasification device experimental data of Figure 2, a plot of  $-\ln[\tau(S)]$  versus the thickness of the POM samples is generated ( $\Delta$  symbols), is shown in Figure 3. (Note that the uncertainties in the thickness and  $-\ln(I/I_0)$  are smaller than the symbol size.) The slope of this line gives the average (integrated over all wavelengths) absorptance  $a$  for the material (POM) for incident radiation with a power distribution given by a blackbody at the source temperature of NIST gasification device (1081 K). As indicated,  $-\ln(\tau(S))$  versus  $S$  is not linear, so the absorption coefficient is not a constant. As indicated in the figure, the slope varies by a factor of nearly four for the range of thicknesses of the measurements. This is in contrast to the data of Jiang et al.<sup>16</sup> for black PMMA, for which measurements over a range of thicknesses of 1 mm to 3.8 mm show a constant slope ( $a$ ). The two points at the value of  $S = 0$

correspond to attenuation from surfaces reflections,  $-\ln(\tau(S)) = -2\ln(1-\rho)$ , with the value of  $\rho$  given from the IS measurement ( $\circ$  symbol) or using the real part of the index of refraction (for visible light),  $n_f = 1.48$  for POM ( $\diamond$  symbol). As indicated, these values agree well with each other. The dotted line in the figure gives the apparent value of the absorptance which one would obtain from a single measurement of the average total transmittance through a 2.9 mm thick slab of POM (using the values of the reflectance as obtained as described above).

To explore this non-linear behavior in more detail, the results of measurements in the IS are presented. Figure 4 shows the total spectral transmittance  $\tau_\lambda(\lambda, S)$  for POM ( $S = 0.027$  mm; right scale) as a function of wavelength; also shown (left scale) is the blackbody hemispherical emissive power,  $e_{\lambda b}(\lambda)$  (note the semi-log scale, and note that  $e_{\lambda b}(\lambda) = \pi i'_{\lambda b}(\lambda)$ ), for source temperatures of 400 K to 2000 K. The IS data are shown for the wavelength range of the instrument (1.5  $\mu\text{m}$  to 15.1  $\mu\text{m}$ ).

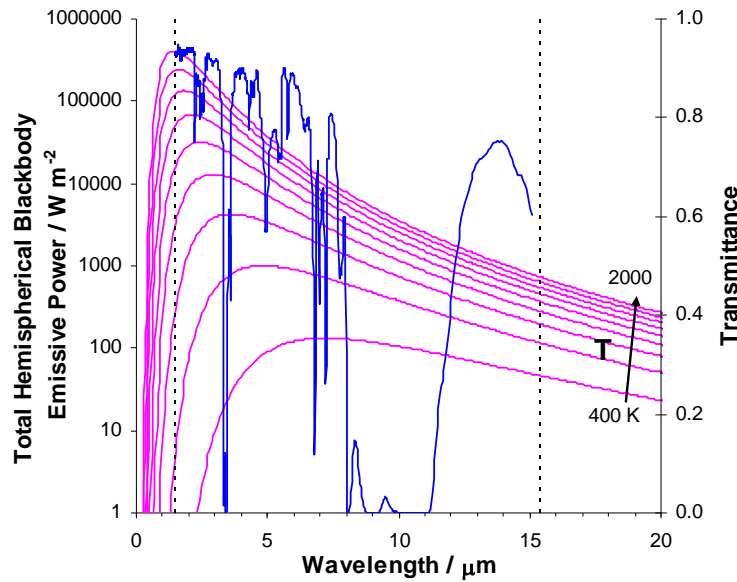


Figure 4– Blackbody hemispherical emissive power as a function of wavelength, for source temperatures of 400 K to 2000 K (left scale), together with transmittance (right scale) for POM ( $S = 0.027$  mm).

From the data in Figure 4, the total average transmittance  $\tau(S)$  is calculated using Eq. 6, assuming a blackbody source temperature the same as the heater in the NIST gasification device (1081 K). Figure 5 shows  $-\ln[\tau(S)]$  in the NIST gasification device ( $\Delta$  symbols, left scale) together with the results in the NIST IS ( $\bullet$  symbols, left scale). As indicated, the agreement between the two methods is excellent for this polymer (and this range of integration of the spectral transmittance). Hence,  $-\ln[\tau(S)]$  as measured with the IS also varies non-linearly with  $S$ . Also shown is the total reflectance ( $\bullet, \circ$  symbols, right scale) for each thickness of sample of POM.

In order to demonstrate the effect of the spectral range of the instrument on the results, we also calculated the transmittance (and reflectance) for a smaller spectral range, 2.5  $\mu\text{m}$  to 15.1  $\mu\text{m}$  (selected because it is a very common range of current Fourier transform Infrared Spectrometers (FTIRs), and has been used in the past by other researchers<sup>7</sup>, whose results have been adopted by others<sup>24</sup>). In Figure 5,  $-\ln[\tau(S)]$  (and the reflectance) are shown as a function of  $S$ , for the smaller spectral range. As indicated, for the narrower spectral range, the curve for  $-\ln[\tau(S)]$  is more nearly linear, with a slope closer to the thin-sample results. Consequently, using the 2.5  $\mu\text{m}$  to 15.1  $\mu\text{m}$  range produces a result which is both

qualitatively and quantitatively different from the 1.5  $\mu\text{m}$  to 15.1  $\mu\text{m}$  results. The reflectance for the thicker samples is 0.04 for the range 1.5  $\mu\text{m}$  to 15.1  $\mu\text{m}$  and 0.03 for 2.5  $\mu\text{m}$  to 15.1  $\mu\text{m}$ ; hence, the effect on the amount of non-reflected energy penetrating the sample, is minor, only about a 1 % discrepancy.

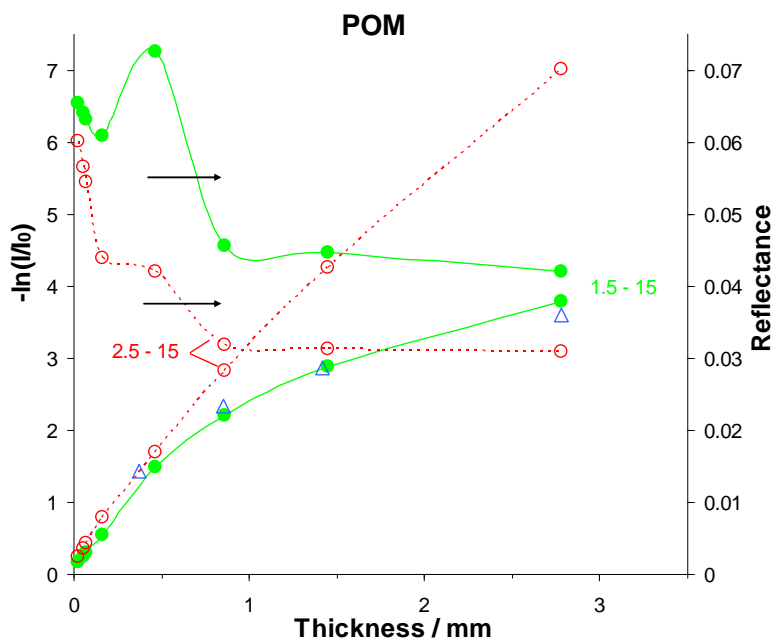


Figure 5 -  $-\ln(I/I_0)$  and reflectance vs thickness for POM (GD and IS).

In order to more fully explore possible non-Bouguer's law absorption behavior by common polymers used in materials fire research, we also examine the absorption and reflection of IR by black Polycast PMMA. This material is selected because it is nearly a standard material in cone-calorimeter studies, and was recently used by Jiang et al.<sup>16</sup> to study the effects of diathermicity on ignition behavior at high flux. In addition to the development and application of an analytic model for predicting the ignition of materials with in-depth absorption of energy, Jiang et al. also measured the transmission of broadband IR through black Polycast PMMA of four thicknesses, and used these to determine the broadband absorption coefficient. The infrared heaters of the FM Global Fire Propagation Apparatus (FPA) were used, in a range of color temperature of 1050 K to 1650 K, which was changed by varying the input voltage to the heaters. The broadband energy transmitted through the samples ( $\approx 1$  mm to 4 mm thick) was detected with a calibrated heat flux gauge.

For comparison with their results, we obtained samples of the Polycast black PMMA (same lot) from the authors of ref.<sup>16</sup>. We pressed them into varying thicknesses (0.090 mm to 3.00 mm), and measured the transmission and reflection of radiation using both the NIST gasification device and the NIST IS. Data were analyzed using the methods described above, and the results are presented in Figure 6. The data in ref.<sup>16</sup> are shown ( $-$  and  $-$  symbols, for source temperature of 1650 K and 1050 K, respectively), with a curve fit (solid line) to the data from all source temperatures. As indicated, the inferred absorption coefficient is  $960.5 \text{ m}^{-1}$  (and there was little variation with source temperature<sup>16</sup>). The data in the present work, taken in the NIST gasification device, are shown by the open triangles. Also shown in the figure are the data from the NIST IS, with the transmission spectrum integrated for a blackbody temperature of 1081 K and a wavelength range of 1.5  $\mu\text{m}$  to 15.1  $\mu\text{m}$  ( $\bullet$  symbols). (For comparison,

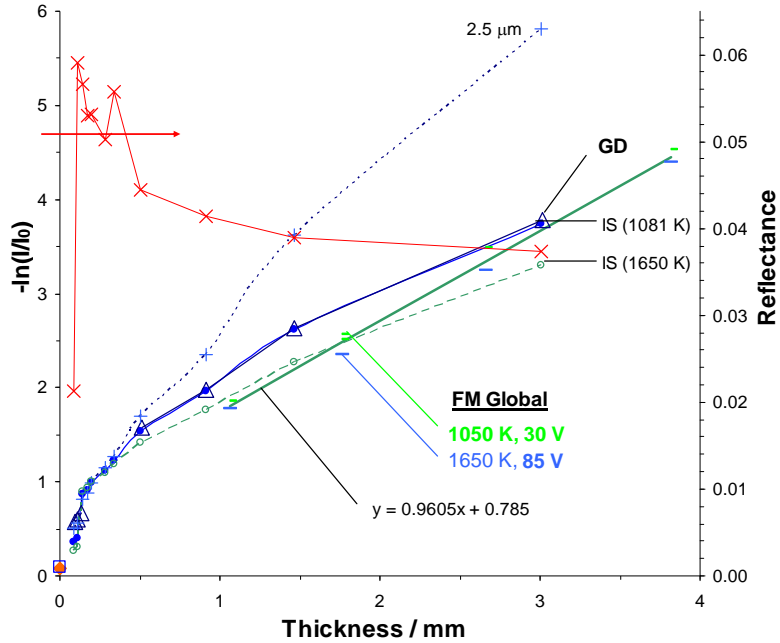


Figure 6  $-\ln(\tau)$  versus thickness for black Polycast PMMA as measured at NIST ( $\Delta$ ,  $\bullet$ ,  $+$  symbols) and at FM Global<sup>16</sup> ( $-$ ,  $-$  symbols).

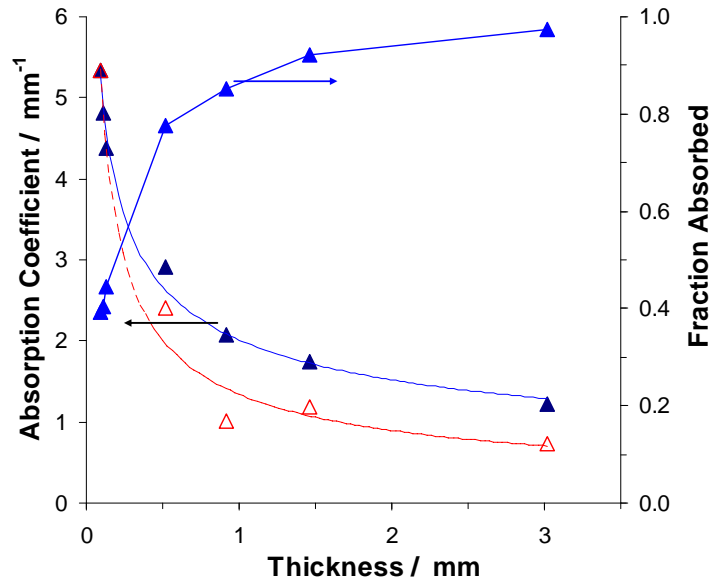


Figure 7 – Absorption coefficient (left scale) for broadband IR as a function of black PMMA thickness (solid line), and the marginal absorption coefficient (dotted line) from the NIST gasification device. Also shown (right scale) is the fraction of energy absorbed for each sample thickness.

data are also shown in which the IS data values of  $\tau_{\lambda}(\lambda, S)$  were converted to the average total transmittance  $\tau(S)$  for a source temperature of 1650 K, to allow comparison with the higher temperature source temperatures in ref. <sup>16</sup>.)

For the black PMMA, the agreement between the NIST gasification device and the NIST IS data is excellent (as was the case for POM). As indicated, for the range of material thickness tested by Jiang et

al. (1 mm to 3 mm), the slope implied by the NIST data (about  $830 \text{ m}^{-1}$ ) is close to that of ref. <sup>16</sup>  $960.5 \text{ m}^{-1}$  (although there is a slight offset in the data). Using the higher source temperature to define the incident radiation to integrate the IS spectral data, the lower IS curve ( $\circ$  symbols) is obtained. The data are very close in magnitude to those of ref. <sup>16</sup>, and although the slope is slightly different ( $a = 720 \text{ m}^{-1}$ ), the agreement not unreasonable given the approximations made throughout. Analysis of the IS data was also performed for a range of integration of  $2.5 \text{ }\mu\text{m}$  to  $15.1 \text{ }\mu\text{m}$  (as indicated by the + symbols in Figure 6); as with POM, for this narrower wavelength range, the results are significantly different from the  $1.5 \text{ }\mu\text{m}$  to  $15.1 \text{ }\mu\text{m}$  results, especially for the larger thicknesses.

Most striking about the data in Figure 6 for black PMMA is that (as was found for POM) the plot of  $\ln[\tau(S)]$  versus  $S$  is non-linear, especially at the smaller thicknesses. To illustrate this effect, Figure 7 shows, for black PMMA, the variation in the absorption coefficient for broadband IR with thickness as calculated using the data in Figure 6 from the NIST gasification device. The absorption coefficient is calculated two ways: as the average value for the thickness of material tested (i.e., the slope of a line from zero thickness up to the point on the curve; solid line, left scale), and as the marginal value based on local slope of the curve (dotted line, left scale). As indicated, for a thin sample (0.1 mm thick), the absorption coefficient is about  $5000 \text{ m}^{-1}$ , and the value drops rapidly as the sample gets thicker. The marginal value of the absorption coefficient drops off somewhat faster, and achieves a lower value at  $S = 3 \text{ mm}$ . Also shown in Figure 7 is the fraction of total energy absorbed as a function of the sample thickness. As indicated, about two thirds of the energy is absorbed within the first 0.33 mm, and the effective absorptivity for that thickness is about  $3200 \text{ m}^{-1}$ . The significance is that while tests with larger thicknesses of material might imply a value of  $a$  near  $1000 \text{ m}^{-1}$ , most of the energy has already been absorbed at smaller thickness, where the effective value of  $a$  is much larger.

## DISCUSSION

There are two ramifications of the results presented above. First, for spectral measurements, it is important to measure the transmission spectra in a wide enough range of wavelengths. Second, for polymers of interest in fire research, the transmission of IR is not described well by Bouguer's law using a constant value of the absorptivity for broadband radiation. These are discussed below.

The required spectral range for accurate description of the absorption of radiant energy depends upon both the blackbody source temperature, as well as the particular spectra of the polymer (as illustrated in Figure 4). To investigate the influence of the former, Figure 8 shows the calculated fraction of the blackbody emissive power<sup>1</sup>) which lies in the wavelength range of either  $1.5 \text{ }\mu\text{m}$  to  $15.1 \text{ }\mu\text{m}$  or  $2.5 \text{ }\mu\text{m}$  to  $15.1 \text{ }\mu\text{m}$ , as a function of the source temperature. In the case of fires, the source temperature of interest would typically be the upper-layer hot gas temperature; in the case of simulating a mass-loss experiment in a laboratory-scale sample<sup>16,25</sup>, the source temperature would be that of the radiant heater used for the experiment. (Temperatures of 500 K to 1100 K in the cone calorimeter, for example, are used to provide a flux of about 5 to 75  $\text{kW}/\text{m}^2$ ); i.e., changing incident fluxes typically employ different blackbody source temperatures, which could affect the absorptance). The arrows indicate the source temperatures for the NIST gasification device as well as the FM Global device used in ref. <sup>16</sup>, along with the value of each curve at that temperature.

As Figure 8 shows, for a radiant source at 1081 K, about 95 % of the blackbody emissive power is within the wavelength range of the NIST IS detector (with about  $\frac{1}{2}$  of the remaining power below  $1.5 \text{ }\mu\text{m}$  and the other half above  $15.1 \text{ }\mu\text{m}$ ). Figure 8 also shows the fraction of energy in the wavelength range of  $2.5 \text{ }\mu\text{m}$  to  $15.1 \text{ }\mu\text{m}$ . While it is highly dependent upon the absorption spectrum of the polymer of interest, the  $2.5 \text{ }\mu\text{m}$  to  $15.1 \text{ }\mu\text{m}$  spectral range would likely be insufficient for radiation from fires. (Note: for plastic glazings in solar collectors, a wider spectral range may sometimes be necessary. In ref <sup>7</sup>, the hottest

source temperature for which calculations were performed was 873 K. At that temperature, nearly 11 % of the blackbody emissive power is below 2.54  $\mu\text{m}$ . Hence, a wider spectrum may be required for the materials described in ref. 7 for a source at 873 K.) Even more important than the blackbody distribution is how a spectra for a particular polymer falls within the blackbody distribution; a range acceptable for one polymer may not be for another. The solution, of course, it to collect spectral data over as wide a range of wavelengths as possible, or use a broad-band technique.

The non-Bouguer's law behavior of the absorbed light for broadband sources is more problematic. It occurs, essentially, because as the incident radiation penetrates the sample, the distribution of energy is no longer that of a blackbody. That is, integration of the spectral transmittance over the blackbody energy distribution is accurate at the surface, but not at depth, where the strong lines have depleted the energy near the spectral regions of high absorption. This has been dealt with in the past though the use of multi-band models of the radiation<sup>26</sup>. The need to do this in sub-grid models of material burning may need to be examined; or perhaps a method based on a non-constant value of the average total absorptivity might be employed.

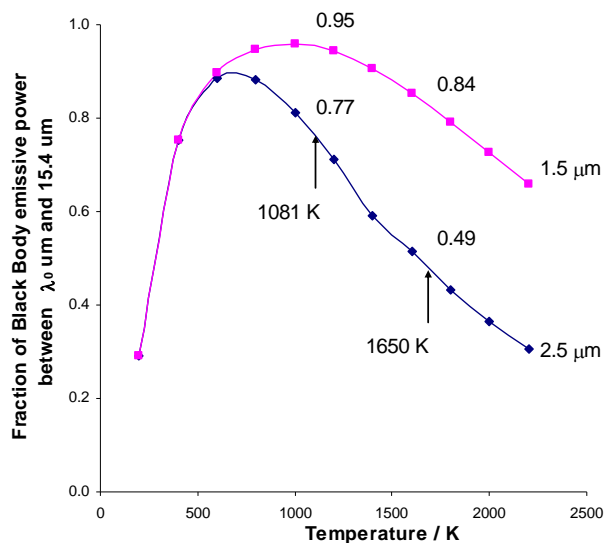


Figure 8 - Fraction of blackbody emissive power between 1.5  $\mu\text{m}$  and 15.1  $\mu\text{m}$  or 2.5  $\mu\text{m}$  and 15.1  $\mu\text{m}$  as a function of source temperature

## CONCLUSIONS

For the thermoplastics PMMA and POM, a radiant source with a broadband thermal detector (e.g., the NIST gasification device, cone calorimeter) can be used to measure the broadband transmission of IR through samples up to 3 mm thick. For these polymers, the method gives nearly identical results for the transmittance as a function of sample thickness as that obtained by measuring the transmittance spectra using the NIST IS, and integrating the transmittance over the blackbody energy distribution at the temperature of the heater. Nonetheless, for use in pyrolysis simulations, the average total absorption coefficient is desired, but for broadband radiation, the average absorptance of these materials was not constant with thickness; the apparent average total absorptance varied by almost an order of magnitude for sample thicknesses between 0.09 mm and 3 mm. Hence, a multi-band description may be required to properly model the penetration of IR into the sample. Also, using the spectral method, an FTIR spectral range of 2.5  $\mu\text{m}$  to 15.1  $\mu\text{m}$  was found to be insufficient for characterizing these materials with respect to IR transmission, while 1.5  $\mu\text{m}$  to 15.1  $\mu\text{m}$  was acceptable for POM and black PMMA (although this will vary with the material and the source temperature).

## ACKNOWLEDGEMENTS

The authors thank John deRis and Mohammed Khan at FM Global, and Stanislov Stoliarov and Rich Lyon of the FAA Technical Center, for helpful conversations and for sending specimens of their material. We are grateful to Takashi Kashiwagi and Ken Steckler at NIST, who performed the experiments in the NIST gasification device, and provided valuable insight.

## REFERENCES

- <sup>1</sup> Siegel, R. & Howell, J.R. 1981. *Thermal radiation heat transfer* Washington, Hemisphere Pub. Corp..
- <sup>2</sup> Katzoff, S. 1965, *Symposium on thermal radiation of solids*, National Aeronautics and Space Administration, Washington, D.C., NASA SP-55.
- <sup>3</sup> Progelhof, R.C. & Throne, J.L. 1971. Determination of Optical Properties from Transmission Measurements. *Applied Optics*, 10, (11) 2548-2549
- <sup>4</sup> Progelhof, R.C., Franey, J., & Haas, T.W. 1971. Absorption Coefficient of Unpigmented Poly(Methyl Methacrylate), Polystyrene, Polycarbonate, and Poly(4-Methylpentene-1) Sheets. *Journal of Applied Polymer Science*, 15, (7) 1803-1807
- <sup>5</sup> Progelhof, R.C., Quintiere, J.G., & Throne, J.L. 1973. Temperature Distribution in Semitransparent Plastic Sheets Exposed to Symmetric, Unsymmetric, and Pulsed Radiant Heating and Surface Cooling. *Journal of Applied Polymer Science*, 17, (4) 1227-1252
- <sup>6</sup> Progelhof, R.C. & Throne, J.L. 1974. Predicting Radiant Energy Transmission Through Polymer Sheets. *Polymer Engineering and Science*, 14, (11) 760-763
- <sup>7</sup> Tsilingiris, P.T. 2003. Comparative evaluation of the infrared transmission of polymer films. *Energy Conversion and Management*, 44, (18) 2839-2856
- <sup>8</sup> Kashiwagi, T. 1981. Radiative ignition mechanism of solid fuels. *Fire Safety Journal*, 3, (3) 185-200
- <sup>9</sup> Kashiwagi, T. 1994. Polymer Combustion and Flammability-Role of the Condensed Phase. *Proceedings of the Combustion Institute*, 25, 1423-1437
- <sup>10</sup> Sohn, Y., Baek, S.W., & Kashiwagi, T. 1999. Transient modeling of thermal degradation in non-charring solids. *Combustion Science and Technology*, 145, (1-6) 83-108
- <sup>11</sup> Drysdale, D. 1998. *An introduction to fire dynamics*, Second ed. Chichester, England, John Wiley and Sons.
- <sup>12</sup> Lautenberger, C. 2010. *A Generalized Pyrolysis Model for Combustible Solids*. Ph.D. (Ph.D. Dissertation). University of California, Berkeley.
- <sup>13</sup> Hallman, J.R., Welker, J.R., & Sliepcevich, C.M. 1976. Ignition times for Polymers. *Polymer-Plastics Technology and Engineering*, 6, (1) 1-56
- <sup>14</sup> Nicolette, V. V., Erickson, K. L., & Vembe, B. E. 2004, Numerical simulation of decomposition and combustion of organic materials, London: Interscience Communications Ltd.

- <sup>15</sup> Stoliarov, S.I., Crowley, S., Lyon, R.E., & Linteris, G.T. 2009. Prediction of the burning rates of non-charring polymers. *Combustion and Flame*, 156, (5) 1068-1083
- <sup>16</sup> Jiang, F.H., de Ris, J.L., & Khan, M.M. 2009. Absorption of thermal energy in PMMA by in-depth radiation. *Fire Safety Journal*, 44, (1) 106-112
- <sup>17</sup> Saito, N., Saso, Y., Ogawa, Y., Otsu, Y., & Kikui, H. Fire Extinguishing Effect of Mixed Agents of Halon 1301 and Inert Gases.
- <sup>18</sup> Linteris, G. 2010. Numerical Simulations of Thermoplastic Pyrolysis Rate: Effects of Property Variations. *Fire and Materials*, ACCEPTED DOI: 10.1002/fam.1066,
- <sup>19</sup> McGrattan, K. B., Klein, B., Hostikka, S., & Floyd, J. 2007, *Fire dynamics simulator (version 5) user's guide*, National Institute of Standards and Technology, Gaithersburg, MD, NIST Special Publication 1019-5.
- <sup>20</sup> Stoliarov, S. I. & Lyon, R. E. 2008, *Thermo-kinetic model of burning*, Federal Aviation Administration, Atlantic City, NJ, Federal Aviation Administration Technical Note DOT/FAA/AR-TN08/17.
- <sup>21</sup> Austin, P.J., Buch, R.R., & Kashiwagi, T. 1998. Gasification of silicone fluids under external thermal radiation part I. Gasification rate and global heat of gasification. *Fire and Materials*, 22, (6) 221-237
- <sup>22</sup> Hanssen, L. 2001. Integrating-sphere system and method for absolute measurement of transmittance, reflectance, and absorptance of specular samples. *Applied Optics*, 40, (19) 3196-3204
- <sup>23</sup> Stoliarov, S.I. & Walters, R.N. 2008. Determination of the heats of gasification of polymers using differential scanning calorimetry. *Polymer Degradation and Stability*, 93, (2) 422-427
- <sup>24</sup> Stoliarov, S.I., Crowley, S., Lyon, R.E., & Linteris, G.T. 2009. Prediction of the burning rates of non-charring polymers. *Combustion and Flame*, 156, 1068-1083
- <sup>25</sup> Twilley, W. H. & Babrauskas, V. 1988, *User's guide for the cone calorimeter*, National Institute of Standards and Technology, Gaithersburg, MD, SP-745.
- <sup>26</sup> Manohar, S.S., Kulkarni, A.K., & Thynell, S.T. 1995. In-Depth Absorption of Externally Incident Radiation in Nongray Media. *Journal of Heat Transfer-Transactions of the Asme*, 117, (1) 146-151